ChemComm

Accepted Manuscript

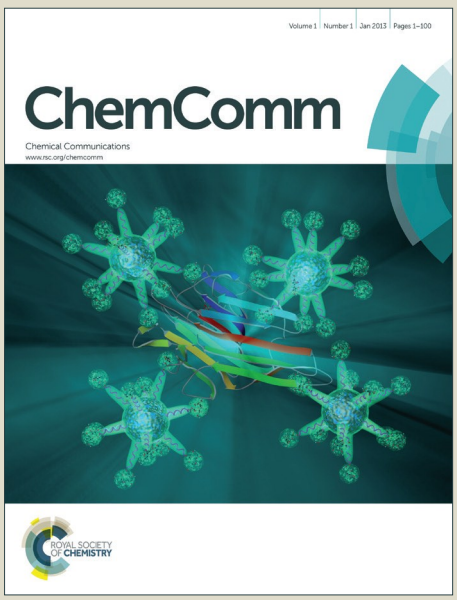

ROYAL SOCIETY OF CHEMISTRY

www.rsc.org/chemcomm

Journal Name

COMMUNICATION

A water-stable metal-organic framework of a zwitterionic carboxylate with dysprosium: a sensing platform for Ebolavirus RNA sequences†

Received 00th January 20xx,

Accepted 00th January 20xx

DOI: 10.1039/x0xx00000x
www.rsc.org/

Liang Qin, Li-Xian Lin, Zhi-Ping Fang, Shui-Ping Yang, Gui-Hua Qiu, Jin-Xiang Chen* and Wen-Hua Chen*

We herein report a water-stable 3D dysprosium-based metal-organic framework (MOF) that can non-covalently interact with probe ss-DNA. The formed system can serve as an effective fluorescent sensing platform for the detection of complementary Ebolavirus RNA sequences with the detection limit of 160 pM.

Ebola Virus Disease (EVD) is an acute virus infection with the high infectivity and high mortality rate.[1] On February 4, 2015, the World Health Organization (WHO) disclosed that there had been totally 22,495 cases of EVD with nearly 9,000 deaths.[2] Ebolavirus are nonsegmented negativesense RNA viruses (NNSVs) that cause severe hemorrhagic fever, and there are no effective vaccines and treatments for this virus infection.[3] Therefore, early diagnosis of Ebolavirus nucleic acid is very important for quarantine and disease control.

At present, one of the effective methods for the detection of Ebolavirus nucleic acid is polymerase chain reaction (PCR), including reverse transcription-PCR (RT-PCR) and real-time quantitative PCR (Q-PCR).[4] This PCR method has received considerable attention because of its rapid analysis.[5] However, its further applications suffer from high cost, risk of contamination and false negative results.[6] Therefore, it is in urgent need to develop more effective approaches for the detection of Ebolavirus RNA.

Guangdong Provincial Key Laboratory of New Drug Screening, School of Pharmaceutical Sciences, Southern Medical University, Guangzhou 510515, China. Email: jxchen@smu.edu.cn (J.-X. Chen); whchen@smu.edu.cn (W.-H. Chen)

†Electronic Supplementary Information (ESI) available: General, synthesis, X-ray crystallography, crystallographic data, selected bond distances and angles, thermogravimetric analysis and 3D structure for **1**. Ebolavirus RNA detection and fluorescence anisotropy experiments. Fluorescence quenching efficiency of P-DNA by compound **1**, H_3CmdcpBr and $Dy(NO_3)_3$ (pH 7.4). Fluorescence intensity of P-DNA@**1** system in the presence of T_0 at varying incubation time (pH 7.4). Fluorescence spectra of the P-DNA@$Dy(NO_3)_3$ system incubated with T_0 of varying concentrations (pH 7.4). Fluorescence spectra of P-DNA incubated with compound **1** of varying concentrations (pH 6.4 and 8.0). Fluorescence spectra of the P-DNA@**1** system incubated with T_0 of varying concentrations (pH 6.4 and 8.0). Fluorescence recovery efficiency of P-DNA@**1** system by T_0, T_1 and T_2 of varying concentrations (pH 6.4, 7.4 and 8.0). CCDC numbers 1417644. For ESI and crystallographic data in CIF format, see DOI: 10.1039/c000000x/.

Metal−organic frameworks (MOFs), readily built from metal ions and organic ligands, are a new class of inorganic materials. The host backbones are composed of metal cation centers and functional organic linkers to produce one, two, or three dimensional extended coordination networks[7] with unique properties, such as sorption,[8] magnetism,[9] luminescence[10] and catalysis.[11] Recently, MOFs have been reported as sensing platforms for biomolecules, including proteins, nucleic acids and antibody.[12] To the best of our knowledge, however, there is no report on using MOF platforms for sensing Ebolavirus RNA.

Herein we report a new 3D dysprosium (Dy) MOF based on a zwitterionic carboxylate ligand *N*-carboxymethyl-(3,5-dicarboxyl)pyridinium bromide (H_3CmdcpBr),[13] that is $\{[Dy(Cmdcp)(H_2O)_3](NO_3)\cdot 2H_2O\}_n$ (**1**), and its high selectivity and sensitivity for the fluorescent detection of Ebolavirus RNA sequences.

Compound **1** was synthesized in a 62% yield from the reaction of $Dy(NO_3)_3\cdot 6H_2O$ with deprotonated pyridinium carboxylate in water at room temperature. Compound **1** is moisture and water stable. The powder X-ray diffraction (PXRD) pattern of a fresh powder of **1** immersed in H_2O for one month, is in agreement with that of the simulated one, indicating its bulky phase purity and water stability (Fig. 1). Thermogravimetric analysis (TGA) indicates that the as-synthesized sample of **1** is stable up to 280 ºC (Fig. S1, ESI†).

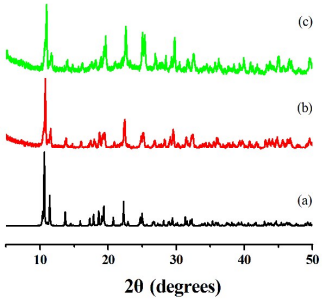

Fig. 1 PXRD patterns of compound **1** showing agreement between the simulated (a), synthesized (b) and fresh powder of **1** immerse in H_2O for one month (c).

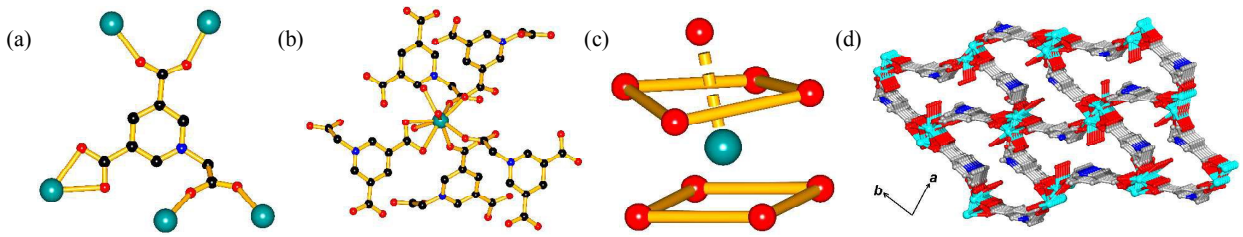

Fig. 2 (a) Linking of the Cmdcp ligand to five Dy centers in a different fashion. (b) The coordination environment of Dy(III) ion. (c) The monocapped square-antiprismatic coordination geometry of Dy(III) ion. (d) The 3D structure of compound **1** viewed down the *c* axis and the free H_2O and NO_3^- were omitted for clarity. Color codes: Dy teal, O red, N blue, C grey.

Compound **1** crystallizes in the monoclinic space group $P2_1/n$ and each asymmetric unit consists of one $[Dy(Cmdcp)(H_2O)_3]^+$ cation, one NO_3^- anion and two free water molecules. As shown in Fig. 2a, the Cmdcp ligand is located on the inversion center and coordinates to one Dy ion in a chelating fashion and to four Dy ions in bridging bidentate coordination fashion. Each Dy center is coordinated by three water molecules, one chelating and four monodentate carboxylates from five Cmdcp ligands (Fig. 2b), thereby forming a monocapped square-antiprism coordination geometry as shown in Fig. 2c. The Cmdcp ligand thus acts as a five-connected node, whereas the Dy center also acts as a five-connected node, leading to a 3D framework (Fig. 2d). The 3D MOF exhibits chair-type pore shapes with tessellating H_2O and free NO_3^- anions on the pore surface (Fig. S2, ESI†).

Because of these unique structural features, compound **1** should, in principle, be able to strongly interact with fluorophore carboxyfluorescein (FAM)-labeled single-stranded DNA (ss-DNA) through π-π stacking, hydrogen bonding and electrostatic interactions, and then quench the fluorescence of FAM.[14] To test this, we chose FAM-5'-CATGTGTCCAGCTGATTGCC-3' as a probe ss-DNA (P-DNA). This sequence is complementary to the part of conservative sequence from Ebolavirus RNA. As shown in Fig. 3a, addition of compound **1** led to a decrease in the fluorescence intensity of P-DNA, suggesting that compound **1** can efficiently quench the fluorescence of P-DNA, possibly *via* the formation of a non-covalent complex (P-DNA@**1** hereafter). It is found that the fluorescence intensity decreases gradually until the concentration of compound **1** reaches 11 μM, indicating saturation for the adsorption of P-DNA. The quenching efficiency (Q_E, %) of P-DNA is 60%, which was calculated *according to* the equation $Q_E\% = (F_0 - F_M)/F_0 \times 100\%$, where F_M and F_0 are the fluorescence intensity at 518 nm in the presence and absence of compound **1**, respectively. In this case, the molar ratio of compound **1** to P-DNA is 220:1. This high ratio may be due to the long chain of FAM-5'-CATGTGTCCAGCTGATTGCC-3' bearing a large FAM tag with dimeter of 9.4 Å, which prevents P-DNA to enter the one-dimensional channels with approximately 8.3×3.3 Å^2 pore aperture. Thus the pore of compound **1** cannot adsorb P-DNA efficiently.

In order to gain further insight into the quenching properties of compound **1**, we measured the quenching efficiency of $Dy(NO_3)_3$ and H_3CmdcpBr toward P-DNA. The data are shown in Fig. S3 (ESI†) and indicate that H_3CmdcpBr result in negligible fluorescence quenching ($Q_E\%$ = 9.4%). In contrast, the presence of $Dy(NO_3)_3$ led to significant quenching ($Q_E\%$ = 85%) with a saturation concentration of 32 μM. These results suggest that $Dy(NO_3)_3$ is also efficient in quenching the fluorescence of P-DNA. This may be a consequence of the intercalation of Dy^{3+} ions into the base pairs of P-DNA and the electrostatic binding with the phosphate backbones,[15] triggering a photoinduced electron transfer (PET) process from FAM to Dy^{3+}.[16]

When the selected Ebolavirus RNA sequences are complementary to the P-DNA sequence, they can form a stable DNA/RNA hybrid duplex. Thus, addition of complementary Ebolavirus RNA sequences to the P-DNA@**1** or P-DNA@$Dy(NO_3)_3$ system may compel P-DNA away from compound **1** or $Dy(NO_3)_3$, leading to the fluorescence regeneration. In such a sense, the P-DNA@**1** and P-DNA@$Dy(NO_3)_3$ systems can serve as a sensing platform for Ebolavirus RNA. This hypothesis was tested by the fluorescence regeneration induced by the addition of Ebolavirus RNA sequences (5'-GGC**A**AUCAGUUGGACACAUG-3', T_0), a complementary target RNA to P-DNA. As shown in Fig. 3b, the fluorescence is recovered upon the addition of T_0 to the P-DNA@**1** system. Interestingly, the fluorescence recovery of the P-DNA@**1** system was found to increase with incubation time and remained unchanged after 120 min (Fig. S4, ESI†). This long recovery time is probably due to the adsorption of P-DNA by the pores of **1** by its non-FAM end as shown in Scheme 1. The big steric hindance of FAM shields the P-DNA re-combination with the Ebolavirus RNA and makes the hybridization difficult. In addition, saturation in the fluorescence recovery was observed at the concentration of 50 nM. Under this condition, the linear relationship between the fluorescence intensity and the concentration of T_0 (inset of Fig. 3b) gave the detection limit of 160 pM, which was calculated from $3\delta_b$/slope (δ_b = standard deviation of five blank measurements). The fluorescence recovery efficiency (R_E) was 0.65, which was calculated using the formula $R_E = F_T/F_M - 1$, wherein F_T and F_M are the fluorescence intensities at 518 nm in the presence and the absence of T_0, respectively. However, the fluorescence of the P-DNA@$Dy(NO_3)_3$ system could not be recovered, presumably due to the strong interaction between Dy^{3+} ion and P-DNA (Fig. S5, ESI†).[15] These results suggest that it is the unique structure of compound **1** that plays an essential role in the fluorescence quenching and regeneration. Specifically, compound **1** forms a complex with P-DNA through multiple non-covalent interactions, in which Dy^{3+} ion play an important role in quenching the fluorescence of P-DNA. Such moderate interactions enable P-DNA to be released from the complex by forming a stable DNA/RNA hybrid duplex with T_0, leading to fluorescence regeneration.[17] Thus, the P-DNA@**1** system can be used as a highly effective fluorescent sensor for Ebolavirus RNA sequences.

Journal Name

COMMUNICATION

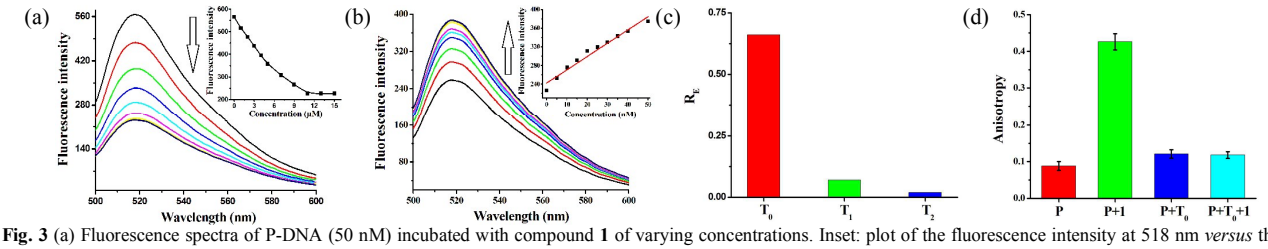

Fig. 3 (a) Fluorescence spectra of P-DNA (50 nM) incubated with compound **1** of varying concentrations. Inset: plot of the fluorescence intensity at 518 nm *versus* the concentrations of compound **1**. (b) Fluorescence spectra of the P-DNA@**1** system (50 nM/11 μM) incubated with T_0 of varying concentrations. Inset: plot of the fluorescence intensity at 518 nm *versus* the concentrations of T_0. (c) Fluorescence recovery efficiency R_E (518 nm) of the P-DNA@**1** system (50 nM/11 μM) by T_0, T_1 and T_2 (50 nM). (d) Fluorescence anisotropy of P-DNA (P, 50 nM) in the presence of compound **1** (11 μM), T_0 (50 nM) and a mixture of T_0 (50 nM) and compound **1** (11 μM) with incubation time of 120 min, respectively. All the tests were conducted in 100 nM Tris-HCl buffer (pH 7.4, 100 mM NaCl, 5 mM $MgCl_2$).

In order to investigate the selective sensing ability of the P-DNA@**1** system, we chose two different target RNAs, that is, one base pair mutated RNA T_1 (5'-GGC**C**AUCAGUUGGACACAUG-3') and non-specific T_2 (5'-GACCAACGTUUAGTCTCAUG-3') to hybridize with P-DNA in the P-DNA@**1** system. Under the same conditions, the R_E is 0.07 for T_1 and 0.02 for T_2, respectively (Fig. 3c). In addition, T_0 shows much higher concentration-dependent fluorescence recovery than T_1 and T_2 (Fig. S6, ESI†). These results indicate that the P-DNA@**1** system can function as a highly selective sensing platform for the detection of Ebolavirus RNA sequences *in vitro*.

In order to further evaluate the selectivity of this sensing system, we conduct the experiment under acidic (pH 6.4) and basic (pH 8.0) conditions. As shown in Table 1 and Figs. S7-S12 (ESI†), under both conditions, compound **1** is efficient in quenching the fluorescence of P-DNA with Q_E% of 65% (pH 6.4) and 77% (pH 8.0), respectively. Meanwhile, the fluorescence of P-DNA@**1** system could be recovered in the presence of T_0 with R_E of 0.27 (pH 6.4) and 0.15 (pH 8.0). Under the same conditions, the R_E is only 0.06 for T_1 and 0.01 for T_2 at pH 6.4, 0.03 for T_1 and 0.02 for T_2 at pH 8.0, indicating that the P-DNA@**1** system can function as a highly selective sensing platform for the detection of Ebolavirus RNA at both pH .6.4 and 8.0. The R_E values at pH 6.4 (0.27) and 8.0 (0.15) are much lower than that at pH 7.4 (0.65). This may be because of that at pH 6.4, FAM exists in neutral or monoanion mode, while at pH 7.4, FAM exists in dianion or trianion mode[18] and exhibits stronger repulsion with NO_3^- in the pores of **1**. Thus the fluorescence of P-DNA is easier to recover at pH 7.4. While at pH 8.0, part of Dy^{3+} in the MOF **1** may form $Dy(OH)_3$ particle,[19] and the fluorescence may be difficult to recover due to the strong interaction between Dy^{3+} ion and P-DNA as we discussed above.

Table 1. The effect of pH on the Q_E% values of compound **1** to P-DNA and R_E values of P-DNA@**1** to T_0, T_1 and T_2

pH	Q_E (%)	R_E for T_0	R_E for T_1	R_E for T_2
6.4	65	0.27	0.06	0.01
7.4	60	0.65	0.07	0.02
8.0	77	0.15	0.03	0.02

The above results may be rationalized from the unique structure of compound **1**. Firstly, compound **1** contains aromatic rings, positively charged pyridinium and Dy^{3+} cation centers, free H_2O and NO_3^- on the pore surface. The zeta potential of +9.0 mV indicates that compound **1** is positively charged.[20] Thus, it is reasonable to deduce that compound **1** can absorb P-DNA through electrostatic, π-stacking and/or hydrogen-bonding interactions to form P-DNA@**1** complex,[21] and thus quench the fluorescence of FAM, in which Dy^{3+} may play a critical role in triggering photoinduced electron transfer (PET) from FAM to Dy^{3+} (Scheme 1).[16]

Secondly, the channel size of compound **1** may play a critical role in effectively distinguishing ss-DNA from DNA/RNA duplex.[22] Because of the large cross-sectional areas and relatively rigid structures, the formed DNA/RNA duplex may not easily enter the pore of compound **1**. In contrast, the smaller cross-sectional areas may make it easier for P-DNA to enter the pore and closely interact with the surface of compound **1**. Thirdly, the most important reason is that compound **1** may has less affinity for duplex DNA/RNA because of the absence of unpaired bases and the rigid conformation of duplex DNA/RNA.[18b] P-DNA is conformationally flexible and should interact with the surface of compound **1** more strongly than rigid duplex DNA/RNA. Therefore, the hybridization of T_0 with absorbed P-DNA would lead to the release of labeled dye with the formed duplex DNA/RNA to the solution, thus resulting in the recovery of fluorescence (Scheme 1).[12f] This is supported by the changes in the fluorescence anisotropy (FA) of P-DNA and P-DNA@T_0 (hybrid duplex DNA/RNA) before and after the addition of compound **1**. It is known that FA can be a measure for the rotational motion-related factors of DNA,[23] and thus provide a means to judge whether P-DNA and P-DNA@T_0 are attached to the surface of compound **1**. As shown in Fig. 3d, the addition of compound **1** into P-DNA leads to an increase in the FA by a factor of 4.8, whereas has negligible influence on the P-DNA@T_0. This result reveals the much stronger interaction of compound **1** with P-DNA than with hybrid duplex DNA/RNA.

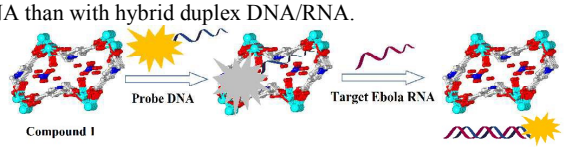

Scheme 1. Mechanism for the target Ebolavirus RNA fluorescent biosensor based on compound **1.**

In summary, we have successfully synthesized and characterized a moisture and water-stable MOF **1** of dysprosium (III) with a zwitterionic carboxylate. Compound **1** can form electrostatic, π-

stacking and/or hydrogen bonding interactions with P-DNA. The formed P-DNA@**1** system can be used as an effective, selective and fluorescent sensing platform for the detection of Ebolavirus RNA sequences. The findings may provide guidance for the synthesis of more metal-zwitterionic carboxylate compounds with potential application in the early diagnosis of Ebolavirus disease.

We are grateful for the financial support from the Guangdong Provincial Department of Science and Technology of China (2015A010105016) and Guangdong Provincial Natural Science Foundation of China (2015A030313284), the National Natural Science Foundation of China (No. 21102070), the Program for Pearl River New Stars of Science and Technology in Guangzhou (No. 2011J2200071) and Southern Medical University.

Notes and references

1. (a) G. K. Goh, A. K. Dunker and V. N. Uversky, *Mol. BioSyst.,* 2015, **11**, 2337; (b) S. Nadhem and H. D. Nejib, *Health. Econ. Rev.,* 2015, **5**, 16.
2. K. Ringen, P. J. Landrigan, J. O. Stull, R. Duffy, J. Melius and M. A. McDiarmid, *Am. J. Ind. Med.,* 2015, **58**, 703.
3. D. W. Leung, D. Borek, P. Luthra, J. M. Binning, M. Anantpadma, G. Liu, I. B. Harvey, Z. Su, A. Endlich-Frazier, J. Pan, R. S. Shabman, W. Chiu, R. A. Davey, Z. Otwinowski, C. F. Basler and G. K. Amarasinghe, *Cell Rep.,* 2015, **11**, 376.
4. (a) V. Salone and M. Rederstorff, *Methods Mol. Biol.,* 2015, **1296**, 103; (b) W. Zheng, Y. Di, Y. Liu, G. Huang, Y. Zheng, Y. Zhang and W. Fang, *Clin. Biochem.,* 2013, **46**, 1566.
5. X. Jiang, W. Jing, L. Zheng, S. Liu, W. Wu and G. Sui, *Lab Chip.,* 2014, **14**, 671.
6. (a) A. Gopi, S. M. Madhavan, S. K. Sharma and S. A. Sahn, *Chest*, 2007, **131**, 880; (b) L. M. Zanoli, R. D'Agata and G. Spoto, *Anal. Bioanal. Chem.,* 2012, **402**, 1759.
7. (a) P. Ramaswamy, N. E. Wong, B. S. Gelfand and G. K. Shimizu, *J. Am. Chem. Soc.*, 2015, **137**, 7640; (b) M. G. Campbell, D. Sheberla, S. F. Liu, T. M. Swager and M. Dincă, *Angew. Chem. Int. Ed. Engl.,* 2015, **54**, 4349. (c) Z. C. Hu, B. J. Deibert and J. Li, *Chem. Soc. Rev.,* 2014, **43**, 5815.
8. (a) C. Pei, T. Ben, Y. Li and S. Qiu, *Chem. Commun.,* 2014, **50**, 6134; (b) A. M. Fracaroli, H. Furukawa, M. Suzuki, M. Dodd, S. Okajima, F. Gándara, J. A. Reimer and O. M. Yaghi, *J. Am. Chem. Soc.*, 2014, **13**, 8863.
9. (a) J. Yang, L. Zhou, J. Cheng, Z. Hu, C. Kuo, C. W. Pao, L. Jang, J. F. Lee, J. Dai, S. Zhang, S. Feng, P. Kong, Z. Yuan, J. Yuan, Y. Uwatoko, T. Liu, C. Jin and Y. Long, *Inorg. Chem.*, 2015, **54**, 6433; (b) D. M. Chen, X. Z. Ma, X. J. Zhang, N. Xu and P. Cheng, *Inorg. Chem.*, 2015, **54**, 2976.
10. (a) D. K. Singha and P. Mahata, *Inorg. Chem.*, 2015, **54**, 6373; (b) B. B. Du, Y. X. Zhu, M. Pan, M. Q. Yue, Y. J. Hou, K. Wu, L. Y. Zhang, L. Chen, S. Y. Yin, Y. N. Fan and C. Y. Su, *Chem. Commun.,* 2015, **51**, 12533.
11. (a) P. García-García, M. Müller and A. Corma, *Chem. Sci.,* 2014, **5**, 2979; (b) H. G. T. Nguyen, N. M. Schweitzer, C. Y. Chang, T. L. Drake, M. C. So, P. C. Stair, O. K. Farha, J. T. Hupp and S. T. Nguyen, *ACS. Catal.,* 2014, **4**, 2496; (c) K. Mo, Y. Yang and Y. Cui, *J. Am. Chem. Soc.,* 2014, **136**, 1746; (d) L. J. Yang, B, B. Tang and P. Y. Wu, *J. Mater. Chem. A,* 2015, **3**, 15838.
12. (a) X. Zhu, H. Y. Zheng, X. F. Wei, Z. Y. Lin, L. H. Guo, B. Qiu and G. N. Chen, *Chem. Commun.,* 2013, **49**, 1276; (b) C. Q. Zhao, L. Wu, J. S. Ren, Y. Xu and X. G. Qu, *J. Am. Chem. Soc.*, 2013, **135**, 18786; (c) H. T. Zhang, J. W. Zhang, G. Huang, Z. Y. Du and H. L. Jiang, *Chem. Commun.,* 2014, **50**, 12069; (d) X. Zhou, W. Zhu, H. Li, W. Wen, W. F. Cheng, F. Wang, Y. X. Wu, L. W. Qi, Y. Fan, Y. Chen, Y. Ding, J. Xu, J. Q. Qian, Z. B. Huang, T. S. Wang, D. X. Zhu, Y. Q. Shu and P. Liu, *Sci. Rep.,* 2015. **5**, 11251; (e) Y. F. Wu, J. Y. Han, P. Xue, R. Xu and Y. J. Kang, *Nanoscale*, 2015, **7**, 1753; (f) L. Chen, H. Zheng, X. Zhu, Z. Lin, L. Guo, B. Qiu, G. Chen and Z. N. Chen, *Analyst*, 2013, **138**, 3490; (g) P. Kumar, P. Kumar, L. M. Bharadwaj, A. K. Paul and A. Deep, *Inorg. Chem. Commun.,* 2014, **43**, 114.
13. (a) J. X. Chen, H. Q. Zhao, H. H. Li, S. L. Huang, N. N. Ding, W. H. Chen, D. J. Young, W. H. Zhang and T. S. A. Hor, *CrystEngComm.,* 2014, **16**, 7722; (b) J. X. Chen, M. Chen, N. N. Ding, W. H. Chen, W. H. Zhang, T. S. A. Hor and D. J. Yong, *Inorg. Chem*. 2014, **53**, 7446.
14. (a) Z. W. Tang, H. Wu, J. R. Cort, G. W. Buchko, Y. Y. Zhang, Y. Y. Shao, I. A. Aksay, J. Liu and Y. H. Lin, *Small*, 2010, **6**, 1205; (b) L. H. Tang, H. X. Chang, Y. Liu and J. H. Li, *Adv. Funct. Mater.,* 2012, **22**, 3083.
15. (a) X. Zhu, H. Y. Zheng, X. F. Wei, Z. Y. Lin, L. H. Guo, B. Qiu and G. N. Chen, *Chem. Commun*., 2013, **49**, 1276; (b) B. Gnapareddy, S. J. Ahh, S. R. Dugasani, J. A. Kim, R. Amin, S. B. Mitta, S. Vellampatti, B. Kim, A. Kukarni, T. Kim, K. Yun, T. H. Labean and S. H. Park, *Colloids Surf. B Biointerfaces*, 2015, **135**, 677.
16. (a) S. X. Jiang, H. Yan and Y. Liu, *ACS Nano*, 2014, **8**, 5826; (b) C. Wang, Y. L. Tang and Y. Guo, *ACS Appl. Mater. Interfaces*, 2014, **6**, 21686; (c) E. K. Lim, T. Kim, S. Paik, S. Haam, Y. M. Huh and K. Lee, *Chem. Rev.*, 2015, **115**, 327; (d) J. Zheng, R. Yang, M. Shi, C. Wu, X. Fang, Y. Li, J. Li and W. Tan, *Chem. Soc. Rev.,* 2015, **44**, 3036; (e) A. P. de Silva, H. Q. Gunaratne, T. Gunnlaugsson, A. J. Huxley, C. P. McCoy, J. T. Rademacher and T. E. Rice, *Chem. Rev.*, 1997, **97**, 1515.
17. (a) B. Rauzan, E. McMichael, R. Cave, L. R. Sevcik, K. Ostrosky, E. Whitman, R. Stegemann, A. L. Sinclair, M. J. Serra and A. A. Deckert, *Biochemistry*, 2013, **52**, 765; (b) J. Li and R. M. Wartell, *Biochemistry*, 1998, **37**, 5154; (c) J. Wang, X. L. Li, J. D. Zhang, N. Hao, J. J. Xu and H. Y. Chen, *Chem. Commun.,* 2015, **51**, 11673; (d) J. Zhang, D. Z. Wu, Q. X. Chen, M. Chen, Y. K. Xia, S. X. Cai, X. Zhang, F. Wu and J. H. Chen, *Analyst*, 2015, **140**, 5082.
18. M. Aschi, A. A. D'Archivio, A. Fontana and A. Formiglio, *J. Org. Chem*., 2008, **73**, 3411.
19. K. Mitsubayashi, K. Nakayama, M. Taniguchi, H. Saito, K. Otsuka and H. Kudo, *Anal. Chim. Acta*, 2006, **566**, 69.
20. (a) R. Deleurence, C. Parneix and C. Monteux, *Soft Matter.*, 2014, **10**, 7088; (b) H. Lakhotiya, K. Mondal, R. K. Nagarale and A. Sharma, *RSC Adv.,* 2014, **4**, 28814; (c) M. Ferriz-Mañas and J. B. Schlenoff, *Langmuir*, 2014, **30**, 8776; (d) A. Mikolajczyk, A. Gajewicz, B. Rasulev, N. Schaeublin, E. Maurer-Gardner, S. Hussain, J. Leszczynski and T. Puzyn, *Chem. Mater.*, 2015, **27**, 2400.
21. (a) Y. Cui, Y. Yue, G. Qian and B. Chen, *Chem. Rev.,* 2012, **112**, 1126; (b) G. Y. Wang, C. Song, D. M. Kong, W. J. Ruan, Z. Chang and Y. Li, *J. Mater. Chem. A,* 2014, **2**, 2213; (c) W. Morris, W. E. Briley, E. Auyeung, M. D. Cabezas and C. A. Mirkin, *J. Am. Chem. Soc*., 2014, **136**, 7261.
22. J. Geng, S. Y. Wang, H. M. Fang and P. X. Guo, *ACS Nano*, 2013, **7**, 3315.
23. (a) L. H. Tang, H. X. Chang, Y. Liu and J. H. Li, *Adv. Funct. Mater.,* 2012, **22**, 3083; (b) J. F. Guo, C. M. Li, X. L. Hu, C. Z. Huang and Y. F. Li, *RSC Adv.,* 2014, **4**, 9379; (c) J. M. Fang, F. Leng, X. J. Zhao, X. L. Hua and Y. F, Li, *Analyst,* 2014, **139**, 801.